ISSN 1674-1056
http://cpb.iphy.ac.cn
http://iopscience.iop.org/cpb
中国物理 B
Chinese Physics
中国物理 Chinese Physics B

Growth and doping of bulk GaN by hydride vapor phase epitaxy

Zhang Yu-Min(张育民), Wang Jian-Feng(王建峰), Cai De-Min(蔡德敏), Ren Guo-Qiang(任国强), Xu Yu(徐俞), Wang Ming-Yue(王明月), Hu Xiao-Jian(胡晓剑), Xu Ke(徐科)
Citation: Chin. Phys. B . 2020, 29(2): 026104 . **doi:** 10.1088/1674-1056/ab65b9
Journal homepage: http://cpb.iphy.ac.cn; http://iopscience.iop.org/cpb

What follows is a list of articles you may be interested in

Electronic and optical properties of GaN-MoS_2 heterostructure from first-principles calculations

Dahua Ren(任达华), Xingyi Tan(谭兴毅), Teng Zhang(张腾), Yuan Zhang(张源)
Chin. Phys. B . 2019, 28(8): 086104 . **doi:** 10.1088/1674-1056/28/8/086104

Control on β conformation of poly(9,9-di-n-octylfluorene) via solvent annealing

Zhi Chao Zhang(张志超), Bing Yue Zhang(张丙悦), Yu Yan Weng(翁雨燕), Tian Hui Zhang(张天辉)
Chin. Phys. B . 2019, 28(7): 076101 . **doi:** 10.1088/1674-1056/28/7/076101

Characterization of structural transitions and lattice dynamics of hybrid organic-inorganic perovskite $CH_3NH_3PbI_3$

Feng Jin(金峰), Jian-Ting Ji(籍建葶), Chao Xie(谢超), Yi-Meng Wang(王艺朦), Shu-Na He(贺淑娜), Lei Zhang(张磊), Zhao-Rong Yang(杨昭荣), Feng Yan(严锋), Qing-Ming Zhang(张清明)
Chin. Phys. B . 2019, 28(7): 076102 . **doi:** 10.1088/1674-1056/28/7/076102

Review of improved spectral response of ultraviolet photodetectors by surface plasmon

You Wu(吴忧), Xiao-Juan Sun(孙晓娟), Yu-Ping Jia(贾玉萍), Da-Bing Li(黎大兵)
Chin. Phys. B . 2018, 27(12): 126101 . **doi:** 10.1088/1674-1056/27/12/126101

Effects of Al component content on optoelectronic properties of $Al_xGa_{1-x}N$

Yan-Jun Ji(纪延俊), Jun-Ping Wang(王俊平), You-Wen Liu(刘友文)
Chin. Phys. B . 2018, 27(10): 106102 . **doi:** 10.1088/1674-1056/27/10/106102

TOPICAL REVIEW — Overcoming doping bottleneck in widegap semiconductors

Growth and doping of bulk GaN by hydride vapor phase epitaxy*

Yu-Min Zhang(张育民)[1,2], Jian-Feng Wang(王建峰)[1,2,†], De-Min Cai(蔡德敏)[2], Guo-Qiang Ren(任国强)[1], Yu Xu(徐俞)[1,2], Ming-Yue Wang(王明月)[1,2], Xiao-Jian Hu(胡晓剑)[1,2], and Ke Xu(徐科)[1,2,‡]

[1] *Suzhou Institute of Nano-tech and Nano-bionics, Chinese Academy of Sciences, Suzhou* 215123, *China*
[2] *Suzhou Nanowin Science and Technology Co., Ltd., Suzhou* 215123, *China*

(Received 31 October 2019; revised manuscript received 14 December 2019; accepted manuscript online 27 December 2019)

Doping is essential in the growth of bulk GaN substrates, which could help control the electrical properties to meet the requirements of various types of GaN-based devices. The progresses in the growth of undoped, Si-doped, Ge-doped, Fe-doped, and highly pure GaN by hydride vapor phase epitaxy (HVPE) are reviewed in this article. The growth technology and precursors of each type of doping are introduced. Besides, the influence of doping on the optical and electrical properties of GaN are presented in detail. Furthermore, the problems caused by doping, as well as the methods to solve them are also discussed. At last, highly pure GaN is briefly introduced, which points out a new way to realize high-purity semi-insulating (HPSI) GaN.

Keywords: GaN, hydride vapor phase epitaxy (HVPE), doping

PACS: 61.72.uj, 81.05.Ea, 81.10.Bk, 61.72.–y **DOI:** 10.1088/1674-1056/ab65b9

1. Introduction

Bulk GaN wafers are widely used as substrates in the growth of laser diodes (LDs),[1,2] the high-power electronic devices,[3–9] and many types of detectors,[10–13] because of the excellent optical and electrical properties.[14,15] Nowadays, commercial bulk GaN substrates are primarily produced by hydride vapor phase epitaxy (HVPE) because of its high growth rate (up to hundreds of micrometers per hour) and the ability to grow large size wafer (up to Φ175 mm).[16–18]

The carrier concentration of undoped GaN grown by HVPE is commonly on the order of 10^{16}–10^{17} cm^{-3},[19] which is unsuitable for GaN-based devices. For example, high conductive GaN substrates ($n > 1 \times 10^{18}$ cm^{-3}) are favored in LEDs and LDs[1] to realize lower resistance and better ohm contact. However, semi-insulating GaN substrates ($\rho > 10^6$ Ω·cm) are preferred in high electron mobility transistors (HEMTs),[3] surface acoustic wave devices,[9,11,20] and particle detectors.[12,21,22] The electrical properties of GaN are mainly controlled by *in situ* doping during the growth. Shallow donors (Si[23,24] and Ge[25,26]), shallow acceptors (Mg),[27] and deep level impurities (Fe[28,29] and C[30,31]) generally serve as the dopants to achieve N-type, P-type, and semi-insulating electrical characteristic of GaN, respectively.

Though the optical and electrical properties of GaN could be improved by doping, the introduction of impurities also causes many problems. At present, Si-related precursors are mostly used in the growth of N-type bulk GaN.[24,32,33] However, the carrier concentration in Si-doped GaN is generally lower than 3×10^{18} cm^{-3}, which is insufficient to further improve the performance of LEDs and LDs. Several factors severely affect the upper limit of Si concentration in GaN, such as the tensile stress induced by dislocation inclination[34,35] and the transition of growth mode due to the anti-surfactant effect of Si impurities.[36,37]

Ge-related precursors are also optional dopants to grow N-type GaN.[38,39] The activation energy is 19 meV and 17 meV for Ge and Si impurities respectively.[40] In addition, the relationship between electron mobility and carrier concentration is similar for Ge and Si doping.[26] Crucially, the formation of Ge_3N_4 is improbable at the growth temperature of GaN (approximately 1040 °C) because it starts to evaporate at temperatures above 600 °C[41,42] and decompose at temperatures above 800 °C.[36] Thus Ge doping could help avoid the deterioration of surface morphology in heavily doped GaN. Nevertheless, whether the stress state of GaN could be affected by Ge doping is still controversial. Fritze *et al.*[36] and Nenstiel *et al.*[43] reported that no tensile stress could be induced by Ge doping, while Xie *et al.*[44] held different opinions. They found that there was obvious tensile stress in Ge-doped GaN, just as the situation in Si-doped GaN. Further-

*Project supported by the National Key Research and Development Program of China (Grant Nos. 2017YFB0404100 and 2016YFA0201101), the National Natural Science Foundation of China (Grant Nos. 61574164, 61704187, and 61604170), the Key Research Program of the Frontier Science of the Chinese Academy of Sciences (Grant No. QYZDB-SSW-SLH042), the State Key Program of the National Natural Science Foundation of China (Grant Nos. 61734008 and 11435010), and the National Key Scientific Instrument and Equipment Development Project, China (Grant No. 11327804).

†Corresponding author. E-mail: jfwang2006@sinano.ac.cn
‡Corresponding author. E-mail: kxu2006@sinano.ac.cn

© 2020 Chinese Physical Society and IOP Publishing Ltd

more, Ge doping could lead to the generation of V-shaped pits in GaN,[36,45] which could lead to the problem of current leakage in Schottky barrier diodes,[46] LEDs,[47,48] and HEMTs.[49] Hence, there are still lots of work to be done to realize high conductive N-type GaN.

In addition, the incorporation of Fe impurities in GaN could also bring about the generation of V-shaped pits. The V-shaped pits are serious defects in Fe-doped GaN which are commonly used as the current blocking layers. But the mechanism of current leakage is unclear, which may be related to deep traps in V-shaped pits[47,49] or unknown conduction mechanisms,[48] and still needs further study.

Moreover, semi-insulating GaN is generally obtained by the compensation of background shallow donors (mainly Si and O impurities) by deep level impurities (mainly Fe and C impurities), but heavy doping leads to tremendous disasters in devices.[50–52] Learning from the experiences in HPSI GaAs[53] and SiC,[54] HPSI GaN points out a new way to solve the problems above. If we could reduce the concentration of the background shallow donors, the concentration of deep level impurities needed to realize semi-insulating electrical characteristic could decrease correspondingly. This could relieve the problems concern with heavy doping. Moreover, highly pure GaN could be used as the drift layer in vertical type power electronic devices, which could greatly increase the thickness of the depletion layer and improve the breakdown voltage.[55] In order to realize HPSI GaN, the background donors should be decreased to less than 1×10^{15} cm^{-3},[56] which is a big challenge.

In this paper, the progress in growth and doping of bulk GaN by HVPE is reviewed. In Section 2, the principles of growth and doping of GaN are introduced. In Section 3 to Section 7, the progresses of unintentionally doped, Si-doped, Ge-doped, Fe-doped, and highly pure GaN are presented respectively. The growth methods, optical and electrical properties, and the defects concern with the corresponding doping, are carefully discussed. Section 8 is a brief summary of the results on GaN doping, and Section 9 is the conclusion of this review.

2. Growth and doping of GaN by HVPE

GaN grown by HVPE method was first reported by Maruska *et al.* in 1969, which was on the foreign substrate of sapphire.[57] Compared with the conventional high-pressure nitrogen solution, Na-flux, and ammonothermal methods, HVPE does not need ultra-high temperature or pressure.[15] In addition, the growth rate of HVPE is up to hundreds of micrometers per hour, which is much higher than the other methods. Moreover, HVPE could grow GaN with high crystal quality as a result of the high thermal stability, high purity, and high surface migration of precursors. However, just because of the high growth rate, HVPE is difficult to grow thin layers. Hence, it is difficult to be used in the growth of device structure, and was not taken seriously at first. But HVPE achieved a rapid development in the 1990 s because of its ability to grow thick bulk GaN wafers.

The schematic diagram of an HVPE equipment is shown in Fig. 1. The HVPE reactor generally contains two zones, namely the source zone (850 °C) and the deposition zone (1040 °C). In the source zone, the Ga source is produced by the reaction of gaseous HCl with metallic gallium to form GaCl gas. Then, the reaction products are transported to the deposition zone by a mixed carrier gas of N_2 and H_2. In the deposition zone, the crystallization of GaN takes place at the substrate area where the gallium source reacts with the nitrogen source (NH_3) at 1040 °C. The growth rate is controlled by the flow rate of HCl gas. The detailed reaction process and the thermodynamic analysis could be found elsewhere.[15]

Because of the lack of native substrate, Si,[58] GaAs,[16] and sapphire,[59] are commonly used as the foreign substrates for the growth of GaN. After growth, the GaN layer could be separated from substrate by thermal etching,[58] chemical etching,[16] or laser lift-off to fabricate bulk GaN[60,61] Because of the big lattice mismatch and thermal expansion mismatch between GaN epilayer and substrate, there is an increase of dislocation density and strain in GaN epilayer. Epitaxial lateral overgrowth (ELOG) could help relieve the stress state and solve the problems above.[62] The mask used in ELOG technology could block the threading dislocations and reduce the dislocation density. In addition, the mask could lead to the bending of dislocations, which further promotes the dislocation reaction and annihilation.[63] Dislocation elimination by inverse-pyramidal pits[64] and nanomask[65] are the improvement of ELOG technology. Besides the methods mentioned above, GaN nanowire arrays fabricated by photoelectrochemical (PEC) etching are almost dislocation- and strain-free, and could be used as the substrate to obtain high-quality and low-strain GaN layer.[66]

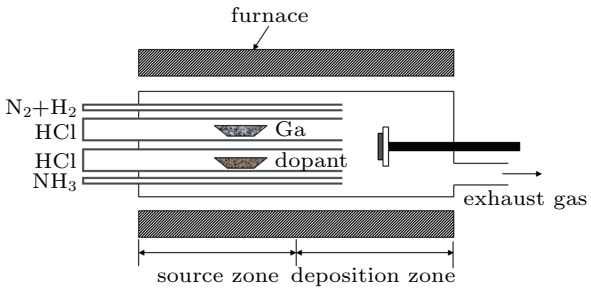


Fig. 1. The schematic diagram of an HVPE system.

Doping in HVPE is more convenient than that in metal organic chemical vapor deposition (MOCVD) or molecular

beam epitaxy (MBE) because of the introduction of HCl gas. HCl gas could react with most of the elemental sources or compounds, so there is no need of the metal organic dopant sources. The doping source is generally produced by the reaction of gaseous HCl with dopant to form chloride gas of dopant in the source zone. Then the doping source is transported to the substrate area by a mixed carrier gas of N_2 and H_2.

The carrier concentration in GaN is mainly determined by the concentration of the incorporated impurity and its ionization ratio. The impurity concentration is influenced by the incorporation efficiency and solubility of the corresponding impurity in GaN. The impurity incorporation efficiency decreases with growth temperature because the vapor pressure of dopants increases with growth temperature. In addition, the large dopant atoms are difficult to be incorporated in GaN due to the relative smaller lattice constant.

The ionization ratio is affected by the activation energy of impurity and the compensation mechanisms. The ionization ratio decreases with the activation energy, leading to a decrease of carrier concentration in wide bandgap semiconductors, because the activation energy of impurity in the wide bandgap semiconductors is relatively larger than that in the narrow bandgap semiconductors. The main compensation mechanisms in GaN are formed by hydrogen atoms, which are introduced into GaN from the carrier gas. The hydrogen atoms could form complexes with the dopants and passivate them.[67] Carbon impurities are also reported to occupy the N site and compensate the shallow donors in GaN.[68] However, the organic sources are unneeded in HVPE. Hence, the carbon concentration in HVPE-grown GaN is much lower than that in MOCVD-grown GaN. Some native point defects (such as the gallium vacancy and the related complexes) are acceptor-like charged centers, which could also compensate the shallow donors.[69]

3. Progress of high-quality undoped GaN

Undoped GaN grown by HVPE generally exhibits the N-type electrical characteristic due to two factors. Firstly, the HVPE reactor is commonly produced by quartz, which could release Si and O impurities to the growth ambience at high temperature. The Si and O impurities are shallow donors in GaN, resulting in the N-type electrical characteristic.[56] Secondly, some native point defects (such as the nitrogen vacancy) are donor-like charged centers, which also contribute to the electrical properties.[69]

It has been reported that dislocation has a great influence on the optical and electrical properties of GaN.[70–72] However, most of the previous studies focused on GaN films grown on foreign substrates by MOCVD or MBE, and thus the dislocation density is very high in these samples. Because of the lack of native substrate, the properties of high-quality bulk GaN were rarely investigated. As we know, the dislocation density decreases with the thickness of GaN.[15] Fortunately, with the development of HVPE technology, we are now able to fabricate thick bulk GaN with dislocation density lower than 1×10^6 cm^{-2}. The optical and electrical properties of high-quality HVPE-grown GaN are carefully studied.

3.1. Scattering mechanisms in high-quality undoped GaN

The schematic diagram of GaN samples sliced from GaN boule grown by HVPE is shown in Fig. 2(a).[19] In accordance with the previously reported results, the dislocation density decreases with the thickness of GaN.[15] Besides, the impurity concentration shows a similar tendency, as shown in Fig. 2(b). Therefore, the thick GaN boule could realize the combination of both high crystal quality and low impurity concentration, and thus its optical and electrical properties could be greatly improved. Figure 2(c) shows the relationship between electron mobility and temperature for the sliced GaN samples. It is found that the mobility of HVPE-grown GaN is as high as 1160 cm^2/(V·s) at room temperature, which is much higher than that of MOCVD-grown GaN.[73]

A model is used to investigate the scattering mechanisms in GaN,[74] in which the influences of ionized impurities, acoustic phonons and dislocations on the electron mobility are all considered.

The mobility due to ionized impurities (μ_i) could be written as

$$\mu_i = \frac{64\sqrt{\pi\varepsilon^2 (2\,kT)^{3/2}}}{N_i e^3 \sqrt{m^*}} \left\{ \ln\left[1 + \left(\frac{12\pi\varepsilon kT}{e^2 N_i^{1/3}}\right)^2\right]\right\}^{-1}, \quad (1)$$

where ε is the permittivity of GaN, k is the Boltzmann's constant, T is the temperature, N_i is the density of ionized impurities, e is the electron charge, and m^* is the effective mass of electrons in GaN.

The mobility due to acoustic phonons (μ_{ac}) could be written as

$$\mu_{ac} = \frac{e\sqrt{8\pi}(h/2\pi)^4 C_{11}}{3\,(E_{ds})^2\,(m^*)^{2.5}\,(kT)^{1.5}}, \quad (2)$$

where C_{11} is the average longitudinal elastic constant of GaN, and E_{ds} is the acoustic deformation potential.

The mobility due to dislocation scattering (μ_{disl}) could be written as

$$\mu_{disl} = \frac{30\sqrt{2\pi}\varepsilon^2 d^2 (kT)^{3/2}}{e^3 N_s f^2 \lambda_d \sqrt{m^*}}, \quad (3)$$

where f is the fraction of the filled traps, N_s is the dislocation density, d is the c-lattice constant of GaN, and λ_d is the Debye screening length.

The total mobility (μ_T) is a result of the comprehensive effect of all the factors above, and can be calculated using the expression below:

$$\frac{1}{\mu_T} = \frac{1}{\mu_i} + \frac{1}{\mu_{disl}} + \frac{1}{\mu_{ac}}. \tag{4}$$

Figure 2(d) shows the contribution of ionized impurities, acoustic phonons and dislocations to the total mobility of HVPE-grown high-quality GaN. It is found that the ionized impurity scattering plays a dominant role in the low temperature range, while the acoustic phonon scattering plays a key role in the high temperature range. Hence, the dislocation scattering plays a nonsignificant role in the entire temperature range. This suggests that the dislocation scattering has little influence on the total mobility of high-quality bulk GaN with dislocation density on the order of 10^6 cm^{-2} or less.

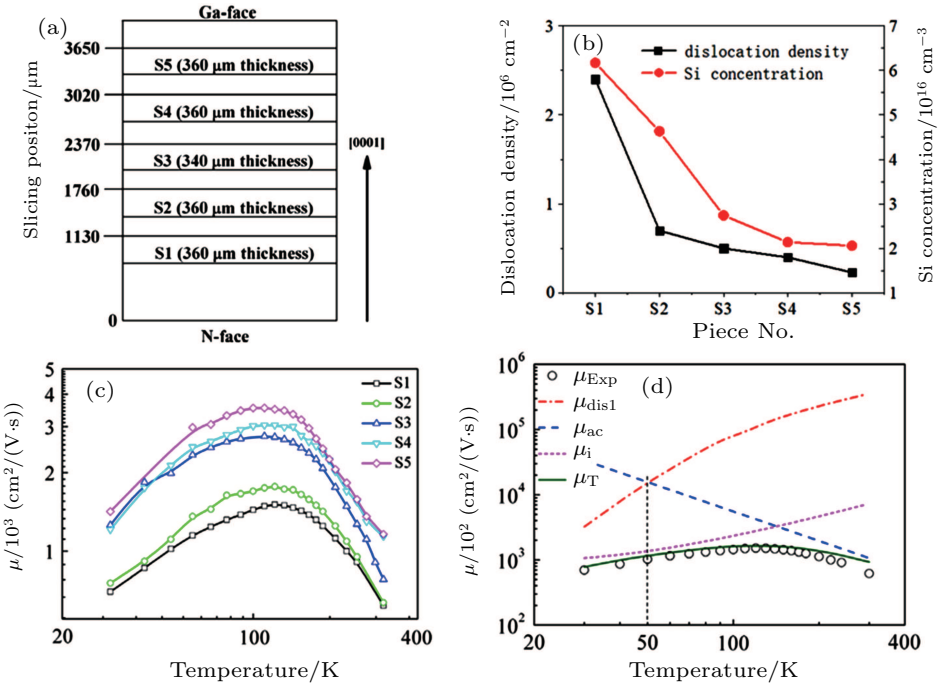


Fig. 2. (a) The schematic diagram of GaN samples sliced from a GaN boule grown by HVPE, (b) the dislocation density and Si concentration for each sample, (c) the relationship between mobility and temperature for each sample, (d) the relationship between mobility and temperature for sample S1. μ_{disl}, μ_{ac}, μ_i indicate the mobility due to dislocations, acoustic phonons, and ionized impurities. μ_{Exp} and μ_T indicate the experimental results and the calculated values according to the model.

3.2. Optical properties of high-quality undoped GaN

A broad yellow luminescence (YL) band with a maximum at approximately 2.2 eV commonly appeared in the PL spectrum of undoped GaN. YL has a great influence on the luminous efficiency of optoelectronic devices,[75] but its origin is still ambiguous. It is recognized as the transition of electrons from conduction band or shallow donors to deep acceptor levels,[76] which may be concerned with C impurity,[77] gallium vacancies,[78] or nitrogen antisites.[79] The previously reported GaN samples were mainly grown on foreign substrates by MOCVD or MBE, and thus the dislocation density and impurity concentration are very high. However, thick bulk GaN grown on native substrate by HVPE could help avoid the above problems and facilitate the study on the mechanism of YL emission.

The photoluminescence spectra of high-quality GaN samples sliced from the bulk GaN crystal are shown in Fig. 3(a). The near band edge (NBE) emission is strong and narrow for all samples, which proves the high crystal quality of HVPE-grown GaN. Moreover, the YL peak intensity decreases with dislocation density while the NBE peak intensity shows a reverse trend.

In order to investigate the influence of dislocation on YL emission, the relationship between Si concentration (N_{Si}) and dislocation density (N_S) is plotted in Fig. 3(b). For comparison, the PL intensity ratio (I_{YL}/I_{BE}) versus dislocation density (N_S) is also shown in Fig. 3(c). The two curves in Figs. 3(b) and (c) both decrease with dislocation density. The YL emission is reported to be related to the transition from shallow donors to deep acceptors.[76] As we know, there are many dangling bonds along the dislocation lines, which could trap the charged impurities.[80,81] During HVPE growth of GaN, the Si impurities could escape from the quartz reactor at high temperature. Then they could be trapped by the dangling bonds around dislocations, and act as shallow donors in the YL emission. Therefore, both the Si concentration and the ratio of I_{YL}/I_{BE} increases with dislocation density. This suggests that, not only the electrical properties, but also the optical properties, could be improved by reducing the dislocation density.

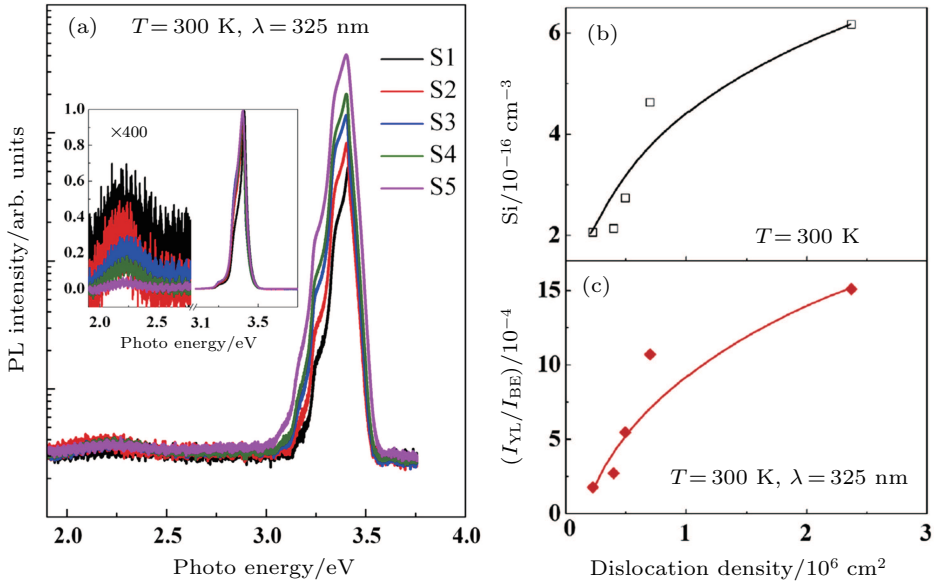


Fig. 3. (a) The room-temperature photoluminescence spectra of GaN samples sliced from the bulk GaN crystal. The inset is the amplified YL band of each sample, which is normalized according to the NBE intensity. (b) The relationship between Si concentration and dislocation density at room temperature. (c) The relationship between I_{YL}/I_{BE} and dislocation density at room temperature.[82]

4. Progress of Si-doped GaN

Low-resistivity GaN substrate is necessary in LED, LD, and power electronic devices to realize better ohm contact and lower threshold voltage. Si doping is commonly adopted to control the electrical properties of GaN. SiH_4 and Si_2H_6 are commonly used as the doping precursors in the growth of N-type GaN by MOCVD or MBE,[32,38] but it is not suitable in HVPE. MOCVD and MBE are cold-wall systems while HVPE is a hot-wall system. The growth temperature of HVPE is typically 1040 °C, which is high enough for the thermal decomposition of SiH_4 and Si_2H_6 gas.[83] After decomposition, nearly all of the Si atoms are deposited on the quartz wall, and contribute less to the N-type doping.

The thermal stability of dichlorosilane (SiH_2Cl_2) is superior to that of SiH_4 or Si_2H_6 gas, and is commonly used in the HVPE growth of Si-doped GaN.[23,24,32,84] Usui *et al.* firstly reported the growth of Si-doped bulk GaN by using SiH_2Cl_2 as the doping precursor, and the carrier concentration could be controlled in the range from 10^{17} cm^{-3} to 10^{18} cm^{-3}.[23] Oshima *et al.* reported that carrier concentration as high as 1.24×10^{19} cm^{-3} could be realized in the growth of Si-doped bulk GaN by HVPE. The electron mobility is approximately 200 cm$^2\cdot$V$^{-1}\cdot$s^{-1}, which is much higher than the MOCVD-grown Si-doped GaN with a similar carrier concentration.[33] Richter *et al.* reported the growth of 2-inch (1 inch = 2.54 cm) Si-doped GaN boule with a thickness exceeding 6 mm.[85]

Moreover, in order to avoid the decomposition of SiH_4 gas at high temperature, solid Si could be used to react with HCl gas to provide the N-type doping source.[86]

In the source zone, HCl gas react with solid Si to form $SiH_{(4-x)}Cl_x$:

$$\mathrm{Si(g)} + x\mathrm{HCl(g)} \rightarrow \mathrm{SiH_{4-x}Cl_x(g)} + (x-2)\,\mathrm{H_2(g)}. \quad (5)$$

After the reaction, the doping source is changed from solid Si into $SiH_{4-x}Cl_x$, which is more stable than SiH_4.

During the transport of doping source to the deposition zone, the following reactions will occur:

$$\mathrm{SiHCl_3\,(g) + H_2\,(g) \rightarrow Si\,(s) + 3HCl(g)}, \quad (6)$$

$$\mathrm{SiHCl_3\,(g) \rightarrow SiCl_2\,(g) + HCl(g)}, \quad (7)$$

$$\mathrm{SiCl_4\,(g) + 2H_2\,(g) \rightarrow Si\,(s) + 4HCl(g)}, \quad (8)$$

$$\mathrm{SiCl_4\,(g) + H_2\,(g) \rightarrow SiHCl_3\,(g) + HCl(g)}, \quad (9)$$

$$\mathrm{SiCl_4\,(g) + H_2\,(g) \rightarrow SiCl_2\,(g) + 2HCl(g)}, \quad (10)$$

$$\mathrm{2SiCl_2\,(g) \rightarrow Si\,(s) + SiCl_4(g)}. \quad (11)$$

Growth temperature has a great influence on the thermodynamic equilibrium composition of the Si/H/Cl system,[87] and further determines the incorporation efficiency of Si impurities.

When $SiH_{4-x}Cl_x$ meets NH_3 in the deposition area, the following reaction happens:

$$4\mathrm{NH_3} + 3\mathrm{SiH_{4-x}Cl_x} \rightarrow \mathrm{Si_3N_4} + 3x\mathrm{HCl} + (12-3x)\mathrm{H_2}. \quad (12)$$

The pre-reaction between NH_3 and $SiH_{4-x}Cl_x$ consumes lots of the doping source, hence the Si concentration in GaN decreases with NH_3 flow rate.

4.1. Scattering mechanisms in Si-doped GaN

The main scattering mechanisms in Si-doped GaN mainly include the ionized impurities, acoustic phonons, and dislocations.[74]

Figure 4(a) shows the curve of mobility versus temperature for two GaN samples with different doping levels. The dislocation density is on the order of 10^6 cm^{-2} for both samples. It is found that there is an obvious discrepancy between undoped GaN ($n\sim1.1\times10^{16}$ cm^{-3}) and Si-doped GaN

($n \sim 6.5 \times 10^{18}$ cm^{-3}). The mobility of the undoped GaN is much higher than that of the Si-doped GaN in the temperature range from 80 K to 300 K, because the ionized impurity scattering in undoped GaN is much lower than that in the Si-doped GaN. For undoped GaN, the ionized impurity scattering is weak, therefore the acoustic phonon scattering plays the main role, and the mobility decreases with temperature in accordance with Eq. (2). However, for Si-doped GaN, the ionized impurity scattering is relatively strong compared with acoustic phonon scattering and plays the predominant role, hence the mobility increases with temperature according to Eq. (1). As a result, undoped and Si-doped GaN show the opposite tendency with temperature.

Figure 4(b) shows the relationship between mobility and carrier concentration at room temperature. Two Si-doped GaN samples with dislocation density of approximately 1.0×10^8 cm^{-2} and 5.0×10^6 cm^{-2} are shown together for comparison. The theoretical curve is also exhibited for reference.[71] It is clearly shown that the mobility of GaN with low dislocation density is superior to that with high dislocation density in accordance with Eq. (3).

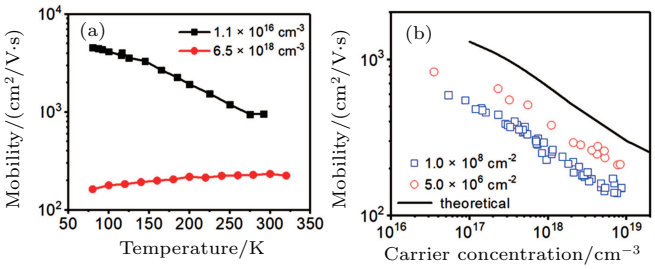


Fig. 4. (a) The relationship between mobility and temperature for GaN with carrier concentration 1.1×10^{16} cm^{-3} and 6.5×10^{18} cm^{-3} respectively. (b) The relationship between mobility and carrier concentration for Si-doped GaN with dislocation densities of 1.0×10^8 cm^{-2} and 5.0×10^6 cm^{-2} respectively. The solid line is the theoretical value of mobility at the corresponding carrier concentration.[71]

4.2. Stress state in Si-doped GaN

A serious problem in Si-doped GaN is the tensile stress resulting from the incorporation of Si impurities, but the mechanism is controversial. Though the covalent radii of Si and Ga atoms are different, the substitution of Ga atoms by Si atoms does not cause obvious changes in the lattice constant according to first-principles calculation results.[88] Therefore the tensile stress does not origin from the difference of covalent radius between Si and Ga atoms. Romano *et al.* reported that the tensile stress increases with Si concentration in GaN, and it is related to the crystallite coalescence process.[88] The prevailing view on the origin of tensile stress is the dislocation inclination caused by the interaction between Si atoms and threading dislocations.[89–91] The inclined dislocations are present in extra-half planes normal to the growth direction, and thus introduce the tensile stress in GaN.

However, the exact mechanism for dislocation inclination is unclear, maybe concern with the following effects: (i) the mask effect due to the formation of SiN_x at the dislocation core;[89] (ii) the prohibition of dislocation movement by Si doping;[92] and (iii) surface mediated dislocation climbing.[93] Xie *et al.* found that the dislocation inclination is caused by the dislocation climb via Ga vacancies.[35] The formation energy of Ga vacancies is controlled by the Fermi level, hence the dislocation inclination is not determined by the Si concentration, but the free carrier concentration.

The strain ($\varepsilon_i^*(z)$) resulting from dislocation inclination could be written as:[34]

$$\varepsilon_i^*(z) = \frac{1}{4} b \rho_{TD} h \tan(\alpha), \tag{13}$$

where b is the Burgers vector, ρ_{TD} is the threading dislocation density, h is the thickness of GaN, and α is the inclination angle.

Because the strain is proportional to TDD according to Eq. (13), a reduction of TDD is necessary to avoid the generation of tensile strain.[94] High-quality facet controlled epitaxial lateral overgrown (FACELO) substrate was reported to be effective in reducing the dislocation density of GaN, and could be used to relieve the tensile stress in Si-doped GaN.[84]

4.3. Anti-surfactant effect of Si in GaN

During the growth of Si-doped GaN, the surface morphology may deteriorate when the Si concentration is too high.[32,36] For heavily Si-doped GaN, the surface is partly passivated due to the deposition of a thin Si_3N_4 layer, which obviously blocks the further growth. Hence, GaN growth occurs only in the regions not covered by Si_3N_4, resulting in the 3D growth mode. This phenomenon origins from the anti-surfactant effect of Si impurities in the growth of GaN.

Munkholm reported that Si atoms tend to segregate to the surface and lead to the change of growth mode from step flow to layer-by-layer at high concentrations.[95] Tanaka *et al.* also found that the growth mode of GaN change from step flow to 3D growth mode when the Si concentration is above 10^{18} cm^{-3}.[96] Neugebauer *et al.* reported that the formation of Si_3N_4 became possible when the Si concentration is high enough, because of the low solubility of Si atoms in GaN. Moreover, the solubility of Si in GaN at N-rich conditions is much lower than that at Ga-rich conditions.[97] Markurt *et al.* found that the mechanism of the anti-surfactant effect of Si impurities could be explained by the formation of a monolayer of $SiGaN_3$ on top of GaN.[37] Density functional theory calculations showed that GaN could not be deposited on this $SiGaN_3$ layer, because the chemical potential at the GaN surface was changed by this layer.

For the Ga-rich condition, the Ga-bilayer structure is the most probable structure, which acts as an auto-surfactant in GaN and could relieve the anti-surfactant effect.[98] Rosa *et al.* reported that the Si atoms tend to segregate to the surface

at N-rich conditions, while they prefer the subsurface sites under Ga-rich conditions.[99] Therefore, Ga-rich condition is preferred in the growth of Si-doped GaN.

5. Progress of Ge-doped GaN

Because of the tensile stress and anti-surfactant effect caused by Si doping, the Si concentration in GaN is limited, and novel dopant sources are needed to further increase the carrier concentration of GaN. Ge related precursors are alternative dopants for the growth of N-type GaN. The activation energy of Ge and Si impurities in GaN are similar, which are 19 meV and 17 meV respectively.[40] Therefore, Ge doping could realize the similar electrical properties as Si doping, and attracts lots of attention recently.[25,26,43]

The doping precursor could be produced by bubbling the carrier gas through liquid $GeCl_4$,[26,45] or the reaction between HCl gas and Ge metal.[25] The Ge concentration increases linearly with $GeCl_4$ feed rate up to 2.4×10^{19} cm^{-3} in the former case,[26] while it increases nonlinearly with the flow rate of HCl gas over the germanium pieces in the latter case.[25] There are mainly two reasons for the non-linearity between Ge concentration and HCl flow rate.[25] Firstly, parasitic deposition of germanium is found at the quartz wall as a result of the decomposition of germanium chloride. The parasitic deposition could reduce the amount of the dopant sources arriving at the substrate, resulting in the non-linearity relationship. An excess of HCl gas could react with the parasitic deposition, and is effective to relieve the problem. Secondly, the reaction area of the Ge metal changes with the reaction time, leading to the variation of the supply of germanium chloride. Hence, a component that could control the reaction area is needed to realize a stable Ge doping.

Oshima *et al.* reported the growth of high-quality Ge-doped bulk GaN crystal with Ge concentration up to 2.4×10^{19} cm^{-3} by HVPE using $GeCl_4$ as the dopant source. The dislocation density kept constant with the increase of Ge concentration, which indicates that the dislocation density is hardly influenced by Ge doping.[26]

In the case of Si-doping, the pre-reaction between NH_3 and $SiH_{4-x}Cl_x$ consumes lots of the doping source, and thus the Si concentration decreases with NH_3 flow rate. However, the pre-reaction between NH_3 and $GeH_{4-x}Cl_x$ is unlikely to occur because of the instability of Ge_3N_4 at the growth temperature. Therefore, NH_3 flow rate has little influence on the Ge concentration in GaN.

Furthermore, just because of the instability of Ge_3N_4 at high temperature, it is unable to affect the growth mode as Si_3N_4.[36] Hence, the surface passivation is unlikely to happen in Ge-doped GaN. Wieneke *et al.* reported that Ge acts as a surfactant in the growth of *a*-plane GaN films, while Si behaves as an anti-surfactant leading to the surface deterioration when Si concentration is above 10^{19} cm^{-3}.[41] Therefore, Ge doping could achieve a higher carrier concentration than Si doping.[43]

5.1. Electrical and optical properties of Ge-doped GaN

The carrier concentration of Ge-doped GaN is nearly identical to the sum of Ge and Si concentration,[26] which indicates that nearly all of the Ge atoms substitute the Ga sites and are ionized at room temperature. This proves the small activation energy of Ge in GaN.[40]

Figure 5 shows the relationship between mobility and carrier concentration at room temperature for Ge- and Si-doped GaN. The dislocation density is on the order of 10^8 cm^{-2} for all the samples. It is found that the electron mobility of Ge-doped GaN decreases with carrier concentration, which is nearly identical to that of Si-doped GaN.[26,100] This means that the electrical properties of Ge-doped GaN is similar to that of Si-doped GaN. Furthermore, the electron mobility for Ge-doped bulk GaN was reported to be much higher than that grown by MOCVD, as a result of the difference in dislocation density and point defect concentration.[26] However, when the carrier concentration is above 1×10^{20} cm^{-3}, Kirste *et al.* found that the mobility remained constant regardless of the change of carrier concentration, because there is a strong screening effect at high carrier concentration.[39]

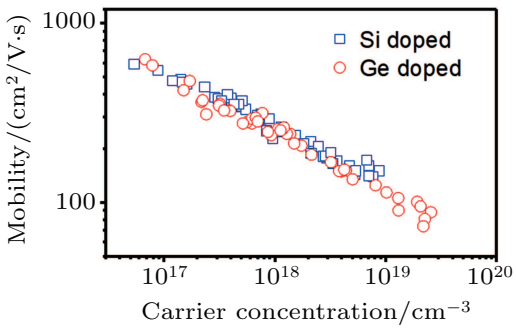


Fig. 5. The relationship between mobility and carrier concentration for Ge- and Si-doped GaN.

Though the carrier concentration increases linearly with the flow rate of Ge source to approximately 2.4×10^{20} cm^{-3},[39] there is an limit of Ge concentration in GaN, which is approximately 2.9×10^{20} cm^{-3}.[36] Further increase of the supply of dopant source does not lead to higher carrier concentration due to two factors. Firstly, the concentration of compensating defects increases at high Ge concentration. Secondly, the solubility of Ge atoms in GaN limits the further increase of Ge concentration. However, the achievable free carrier concentration of Ge-doped GaN is much higher than that of Si-doped GaN. This enhanced doping capability of Ge-doped GaN could facilitate its application in plasmonic detectors.[39]

The optical properties of Ge-doped GaN is influenced by the doping level. Figure 6 shows the low-temperature photoluminescence spectrum of a heavily Ge-doped GaN with a carrier concentration of approximately 2.6×10^{19} cm^{-3}. There are two peaks in the NBE emission band. The sharp peak centered at 3.472 eV is recognized as a localized center concern with germanium atoms.[39,101] The broad peak with an FWHM of hundreds of meV is influenced by two effects. The low energy side is influenced by the bandgap renormalization effect as a result of the impurity scattering and Coulomb interaction of the electrons.[102] The high energy side of the broad peak is determined by the Burstein–Moss effect caused by the band filling.[103]

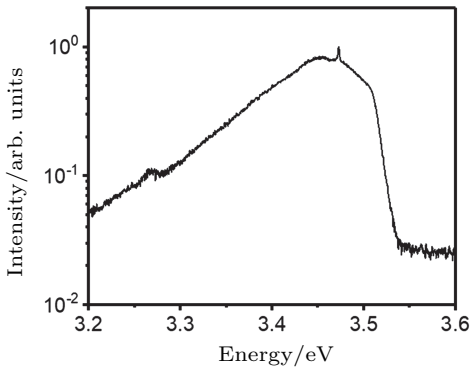


Fig. 6. Low temperature (4 K) photoluminescence spectrum of GaN with Ge concentration approximately 2.6×10^{19} cm^{-3}.

5.2. Stress state in Ge-doped GaN

It is well known that Si doping could result in tensile stress in GaN, but whether Ge doping could influence the stress state is still controversial. The tensile stress in Si-doped GaN is widely considered to be due to the dislocation inclination caused by dislocation climb.[34,36,44,90,93,104,105] One commonly accepted view on dislocation climb is the masking effect of Si_3N_4, which is assumed to mask the dislocation core during the growth.[36,89] According to this model, the strain is determined by the Si concentration only. In the case of Ge doping, Ge_3N_4 decomposes at temperatures above 900 °C, so it is unlikely to mask the dislocation core. In accordance with this view, several groups have reported that Ge doping does not alter the strain state even in highly Ge-doped GaN layers in comparison with Si doping.[36,41,43,106]

However, Xie *et al.* reported that the strain in Si-doped GaN films is not determined by the Si concentration, but the free carrier concentration.[35] According to this model, the edge type dislocations could climb through Ga vacancies. The formation energy of the negatively charged Ga vacancy decreases with Fermi level, which is further determined by the carrier concentration. From this point of view, Ge doping and Si doping have the similar effects on the stress state in GaN. However, up to now, the influence of Ge doping on the stress state, as well as the interaction between dislocations and point defects, still needs further study.

5.3. V-shaped pits in Ge-doped GaN

Nakamura *et al.* reported that there were many pits on the surface of heavily Ge-doped GaN films grown by MOCVD.[38] But the situation is controversial in HVPE. Hofmann *et al.* found that few pits appeared on the surface of Ge-doped GaN with a carrier concentration of approximately 2.6×10^{17} cm^{-3},[25] while Fritze *et al.* reported that some pits emerged on the surface of Ge-dopd GaN. The pits could be prevented by improving the quality of GaN buffer because they were related to the screw-type dislocations.[36] Oshima *et al.* realized the growth of Ge-doped GaN without any pits.

Iwinska *et al.* found that H_2 has a great influence on the generation of pits.[45] The influence of H_2 on the equilibrium partial pressure of Ge is analyzed by thermodynamic calculations.[45] The corresponding chemical reactions are shown below:

$$H_2 + Cl_2 = 2HCl, \tag{14}$$

$$GeCl_4 + H_2 = GeCl_2 + 2HCl, \tag{15}$$

$$GeCl_2 + H_2 = Ge + 2HCl, \tag{16}$$

$$Ge + H_2 = GeH_4, \tag{17}$$

$$GaCl + NH_3 = GaN + H_2 + HCl, \tag{18}$$

$$GaCl + 2HCl = GaCl_3 + H_2. \tag{19}$$

According to the calculation results, the equilibrium pressure of Ge is higher than the saturated vapor pressure of Ge in the H_2 ambient at the growth temperature, hence the Ge atoms tend to aggregate to form droplets. The droplets are foreign particles, which could lead to the formation of pits.[107] With the increase of N_2 partial pressure, the equilibrium pressure of Ge decreases rapidly to lower than its saturated vapor pressure. Therefore, growth in the pure N_2 ambience is an efficient method to prevent the formation of pits.

6. Progress of Fe-doped GaN

Semi-insulating GaN substrates are widely used in high power and high frequency devices,[52,108] due to the excellent properties of high resistivity and high breakdown voltage.[15] However, undoped GaN generally shows N-type conductivity due to the residual donor impurities such as O and Si.[109] In order to fabricate semi-insulating GaN, Fe impurities are commonly adopted to compensate the residual impurities,[15] because Fe impurities are deep level acceptors in GaN.

$FeCl_2$ (produced by the reaction between metallic Fe with gaseous HCl)[28,109] or ferrocene (Cp_2Fe)[29,110] was reported to be employed as the dopant sources. The Fe concentration increases linearly with the partial pressure of HCl gas passing through the Fe metal in the former case,[109] while it increases super-linearly with the flux of ferrocene in the latter case.[29] The enhanced incorporation efficiency at the surface steps was

used to explain the super-linearity. In addition, Fe concentration in GaN decreases with growth rate,[29] which reflects the mass transport limitation of Fe impurities in GaN.

GaN with Fe concentration as high as 2×10^{20} cm^{-3} was reported by Malguth *et al.*[111] Richter *et al.* succeeded in the fabrication of 3 inch Fe-doped GaN with a thickness of 1 mm. No significant impact on the crystalline quality was observed for Fe levels up to 2×10^{18} cm^{-3}.[29]

Fe concentration shows a slow turn-on and turn-off at the point of the start and end of the doping process. Heikman *et al.* found that, contrary to the memory effect in Mg doped GaN,[112] this problem originates from the Fe segregation on the sample surface.[113] Oshimura *et al.* reported that, even when the Fe precursor is cut off, Fe impurities could also be incorporated into the undoped GaN via solid phase diffusion, surface segregation, or vapor diffusion.[52] Therefore, it is difficult to realize a well-defined profile with a sharp turn-on and turn-off in Fe-doped GaN. An improved turn-off profile could be achieved by etching the Fe-doped GaN substrate in acids prior to the subsequent growth.[113]

6.1. Electrical properties of Fe-doped GaN

The resistivity of Fe-doped GaN is controlled by the compensation of the unintentionally doped shallow donors by Fe impurities, so it increases with Fe concentration and decreases with the donor concentration. Hence, by reducing the background Si and O concentration, the Fe concentration that needs to realize the semi-insulating electrical characteristic decreases substantially.

Heikman *et al.* reported that both carrier concentration and mobility decreases with Fe concentration.[113] For the lightly doped samples, the carrier concentration decreases with Fe concentration at a constant negative slope of 0.34, which means that each Fe atom could trap 0.34 free electrons on average. The Hall mobility shows a $T^{-2.2}$ dependency with temperature as a result of the optical phonon scattering.[29]

Vaudo *et al.* reported that the resistivity of Fe-doped GaN sharply decreased with temperature.[28] This indicates that the electrons captured by Fe impurities could escape at high temperature. According to the relationship between carrier concentration and temperature (n *versus* $1/T$), the activation energy could be obtained. It was found that the activation energy of Fe-doped GaN is much higher than that of the undoped GaN,[29] which also confirms that an increasing number of free electrons generate at elevated temperatures. The activation energy could also be derived from the relationship between resistivity and temperature (ρ *versus* $1/T$), which was similar to that obtained from the relationship between carrier concentration and temperature (n *versus* $1/T$).[29]

6.2. Structural and electronic properties of Fe in GaN

The Fe atoms commonly occupy the Ga sites in the GaN lattice. Fe atoms incorporated into GaN have a co-existence charge state of Fe^{2+} and Fe^{3+}, and introduce a charge transfer level ($Fe_{Ga}^{3+/2+}$) in the band gap.[114] The charge transfer level is controversial, which was reported to be 2.6 eV,[115] 3.17 eV,[116] or 2.863 eV[114] above the valence band maximum. Because the charge state of $Fe_{Ga}^{3+/2+}$ is transferred from Fe_{Ga}^{3+} to Fe_{Ga}^{2+} by capturing an electron, the Fe atom acts as a compensating deep acceptor in GaN, resulting in the semi-insulating electrical characteristic of Fe-doped GaN. The Fermi level moves from near the conduction band to the $Fe^{3+}/^{2+}$ charge-transfer level with the increase of Fe doping level. However, when the Fe concentration is above 1×10^{19} cm^{-3}, further increasing the Fe concentration does not induce the change of Fermi level, because it is pinned at the $Fe_{Ga}^{3+/2+}$ charge-transfer level.[114]

The d^5 configuration of Fe^{3+} on the Ga site is split into the ground state $^6A_1(S)$ and the excited states of $^4T_1(G)$, $^4T_2(G)$, and $^4E(G)$ as a result of the impact of the ligand field, while the d^6 configuration of Fe^{2+} is split into the states of ^5E and $^5T_2$,[116] as shown in Fig. 7. Because the[5] T_2 state was considered to be degenerated with the conduction band,[117] it is not shown here.

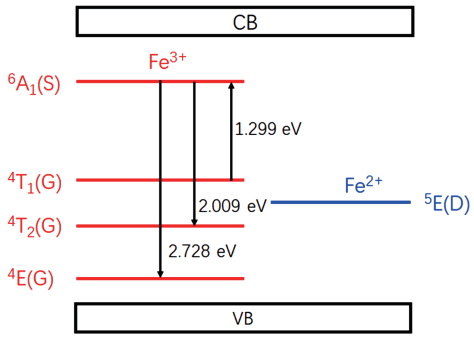


Fig. 7. Schematic diagram of the energy level of Fe^{3+} and Fe^{2+} in Fe-doped GaN.

6.3. Optical properties of Fe-doped GaN

Figure 8(a) shows the typical photoluminescence spectra of Fe-doped GaN with Fe concentration of approximately 1×10^{18} cm^{-3}.[118] Four sharp lines appear in the near-IR range of 1.2 eV–1.3 eV, which originate from the transitions from the crystal-field split $^4T_1(G)$ state to the $^6A_1(S)$ ground state of the Fe^{3+} center. The enlarged luminescence spectrum in the near-IR region is shown in Fig. 8(b). The lines in the range of 1.20 eV–1.28 eV are the vibrational replicas of the line at 1.299 eV.[110] These lines broaden with the increase of temperature, and merge into a broad PL band at room temperature.[110]

The enlarged NBE luminescence spectrum is shown in Fig. 8(c). The free exciton A (FX_A), free exciton B (FX_B),

donor bound exciton (DBE), and acceptor bound exciton (ABE) emissions could be observed at 3.486 eV, 3.492 eV, 3.480 eV, and 3.474 eV respectively.[118] The intensity of the NBE emission decreases with Fe concentration, and are quenched when the Fe concentration is high enough. According to the relationship between NBE intensity and Fe concentration, we could roughly evaluate the Fe concentration.

The defect-related broad YL band is very weak in Fe-doped GaN, because the incorporation of Fe into GaN could quench YL.[110] It was reported that the Fermi level shifts from near the conduction band to near the midgap with the increase of Fe doping level.[114] Because the formation energies of point defects and the related complexes are influenced by Fermi level,[69] the Fe doping level has a great influence on the sub-bandgap emission.

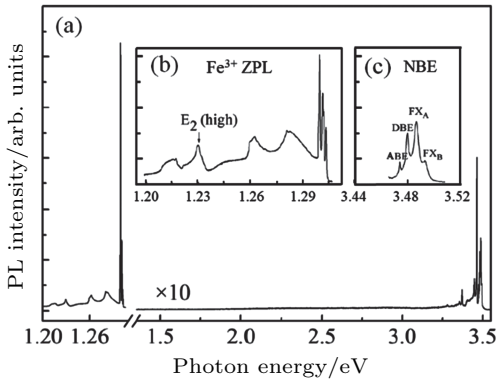


Fig. 8. (a) Typical PL spectrum of Fe-doped GaN. The enlarged spectrum is shown in panel (b) the near-IR region and (c) the NBE region.

6.4. V-shaped pits in Fe-doped GaN

V-shaped pits commonly appear in large numbers on the surface of Fe-doped GaN. The origin of V-shaped pits may be related to the strain caused by transition metal doping.[111] Fe-doped semi-insulating GaN wafers are generally used as the current blocking layers in devices, while V-shaped pits are commonly recognized as the current leakage channels in GaN, hence V-shaped pits are harmful to the performance of devices.

Even though the V-shaped pits could be removed by a chemical mechanical polishing process (CMP), the current leakage channels still exist in the crystal bulk, as shown in Fig. 9.[119] Though the surface is flat after the CMP process (Fig. 9(b)), there is a pit halo with high carrier concentration in the optical microscope image (Fig. 9(a)) and the cathodoluminescence image (Fig. 9(c)).

Figure 9(d) shows the Raman spectra across a pit halo. The LOPC mode origins from the coupling of free carriers with the A_1(LO) vibrational mode, and could be used for the calculation of carrier concentration.[14] It is found that the longitudinal optical phonon-plasmon coupled (LOPC) mode appears in most of the Raman spectra, and varies at different positions of the pit halo, as shown by the arrows in Fig. 9(d). Figure 9(e) shows the distribution of carrier concentration across a pit halo. The carrier concentration outside and near the center of a pit halo is too low to be detected, they are not shown. It is found that the carrier concentration in the pit is much higher than that out of the pit. In the pit, the carrier concentration is not uniform, and continuously increases from center to the edge.

The nonuniform distribution of carrier concentration leads to a nonuniform distribution of resistivity. In Fig. 9(f), scanning spreading resistance microscopy (SSRM) measurement shows that the resistance in the edge of a pit is approximately 5 orders of magnitude lower than the normal area. Hence the pit is the main current path because of its high conductance, resulting in the problem of current leakage.

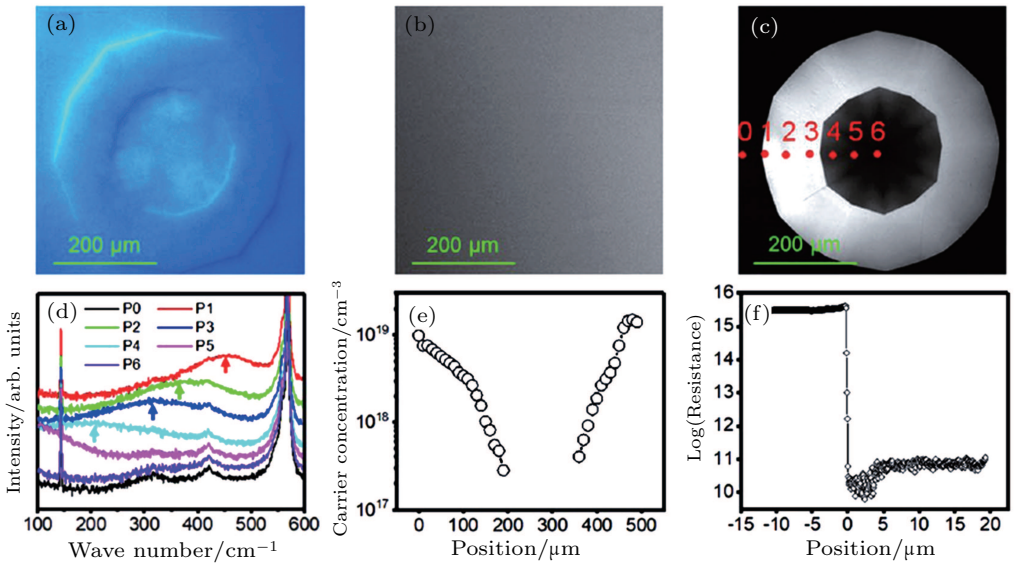


Fig. 9. (a) OM, (b) SEM, and (c) CL image of a pit halo, respectively. (d) Raman spectra at typical positions of a pit halo. The points labeled as P0–P6 are shown in Fig. 1(c). (e) The carrier distribution in a pit halo. The ordinate origin refers to the left edge of a pit halo. (f) The resistance distribution near the edge of a pit halo. The ordinate origin refers to the left edge of a pit halo.

The optical properties in the pit is also influenced by the high carrier concentration. The NBE intensity in the pit is approximately four orders of magnitude higher than that in the normal area.[111] When the carrier concentration is above the critical Mott density, the position and shape of the NBE peak will change as a result of the Burstein–Moss effect[120] and band-gap renormalization.[121]

The variation of carrier concentration in the pit halo indicates a nonuniform distribution of impurities. Secondary ion mass spectroscopy (SIMS) line mapping across a pit halo shows that the high carrier concentration mainly originates from the high incorporation of O and Si impurities. The growth face is Ga-polar (0001) plane in the normal area, while it is semi-polar (10–11) plane in the V-shaped pits. The semi-polar growth facets significantly enhance the incorporation efficiency of Si and O impurities,[122,123] resulting in the higher Si and O concentrations. Furthermore, the incorporation efficiency of the compensative Fe impurities is lower in the V-shaped pits than the normal area. Hence the net carrier concentration further increases in the V-shaped pits.[119]

7. Progress of highly pure GaN

The background donors are harmful to the performance of bulk GaN substrates. In order to fabricate semi-insulating GaN substrates, lots of Fe impurities should be incorporated into GaN to compensate the background donors. Therefore, various problems concern with Fe impurities may occur. It was reported that the GaN/AlGaN HEMTs suffer from serious current collapse caused by the Fe_{Ga}–V_N complex.[50] In addition, the recovery time of the low noise amplifiers is longer for the transistors with Fe-doped buffer than those with unintentionally doped buffer, as a result of the trapping effect of Fe impurities.[51] Furthermore, the Fe impurities in the substrate could easily diffuse into the channel region of the device and have a great influence on the device performance.[52]

The unintentionally incorporated impurities are harmful to the performance of GaN-based devices. The drift layer of vertical power electronic device should be highly pure to improve the breakdown voltage and reduce the leakage current. However, the highly pure epitaxial layer is difficult to grow by MOCVD because there are many carbon impurities from the metal–organic sources.[55,124] In HVPE growth of GaN, carbon-free precursors (Ga metal and NH_3) are used, and thus the carbon concentration in the HVPE-grown GaN is much lower than the MOCVD-grown GaN.[125]

Moreover, the thickness of drift layer in GaN-based power device is generally above 10 μm, therefore HVPE is superior to MOCVD because of its high growth rate. The absence of carbon impurities and high growth rate make HVPE an excellent choice for the growth of thick drift layers in the application of power electronic devices. However, the unintentionally doped GaN grown by HVPE commonly exhibits N-type electrical characteristic with carrier concentration ranging from 10^{16} cm^{-3} to 10^{17} cm^{-3}.[17] The high background donor concentration could greatly reduce the width of the depletion region, resulting in a large decrease of the breakdown voltage.[55,126,127] Therefore, the reduction of Si and O concentration is a big challenge in the growth of highly pure GaN by HVPE.

The highly pure GaN crystal with a resistivity above 1×10^9 Ω·cm could be achieved by reducing the concentration of background donors.[17] All the measured impurities are below the corresponding detection limit, hence the concentration of Si or Mg impurities that needed to realize N-type or P-type electrical characteristic decreases substantially. These progresses suggest that HVPE is superior to MOCVD in the growth of power electronic device structures.

7.1. Origin of the background impurities

Fujikura *et al.* reported that the concentration of Si and O could be controlled below the detection limit of SIMS by a quartz-free HVPE equipment.[17] This suggests that the Si and O impurities in the HVPE-grown GaN mainly come from the quartz parts of the HVPE reactor. At the growth temperature (approximately 1040 °C), HCl and NH_3 gas could react with quartz and release the Si and O impurities to the vapor phase.

7.2. Influence of polarity on the incorporation efficiency of impurities

It was reported that the impurities are more readily incorporated into the N-polar GaN films.[123,128] This suggests that the polarity of growth facet has a great influence on the incorporation efficiency of impurities in GaN. The influence of polarity on the incorporation efficiency of Si is weak.[123] Xu *et al.* reported that under the same growth conditions, the Si concentration in the polar, nonpolar, and semi-polar face samples are nearly identical.[122] However, the incorporation efficiency of oxygen on the (000–1) facet is much higher than that on the (0001) facet. Therefore, in order to reduce the oxygen concentration in GaN, it is preferable to grow on the (0001) facet. The mechanism for the high incorporation efficiency of O impurities on the (000–1) facet is shown below:

Firstly, the adsorption energy of oxygen impurities on the (0001) facet decreases with oxygen coverage, reflecting a strong repulsive interaction between the oxygen atoms on the (0001) facet.[129] As a result, the oxygen impurities could hardly be incorporated into the (0001) facet. However, for the (000–1) facet, the situation is qualitatively different. Sumiya *et al.* reported that oxygen incorporation on the N face was 100 times higher than that on the Ga face.[128]

Secondly, the density of dangling bands on the (000–1) facet is much higher than that on the (0001) facet.[130] Fichtenbaum *et al.* found that the oxygen atom occupying the N site could form only a single bond to the surface atoms on the (0001) facet, while it could form 3 bonds to the surface atoms on the (000–1) facet.[131] Hence the N face provides more sites for impurity incorporation.

8. Summary of the results on GaN doping

The growth and doping of bulk GaN by HVPE achieve great development as a result of the hard work from scientists and engineers, but there are still some remaining problems needed to be solved. The following table shows the progresses and challenges in growth and doping of bulk GaN by HVPE.

Table 1. The progresses and challenges in growth and doping of bulk GaN by HVPE.

Doping type	Dopant source (or the growth method)	Impurity concentration	Electrical properties	Main challenge(s)
Si doping	1) SiH_2Cl_2 2) Si + HCl	10^{19} cm^{-3}	Carrier concentration: 10^{19} cm^{-3}	1) Tensile stress 2) Anti-surfactant effect
Ge doping	1) $GeCl_4$ 2) Ge + HCl	10^{19} cm^{-3}	Carrier concentration: 10^{19} cm^{-3}	1) Tensile stress 2) V-shaped pits
Fe doping	1) Cp_2Fe 2) Fe + HCl	10^{20} cm^{-3}	Resistivity: 10^{11} Ω·cm	V-shaped pits
Highly pure	Remove quartz parts from high temperature region	[Si] $< 5 \times 10^{14}$ cm^{-3}, all the impurities are below their relevant detection limits.	Resistivity: $> 1 \times 10^{9}$ Ω·cm	Quartz-free HVPE reactor

9. Conclusion

The commercial native GaN substrate is mainly produced by HVPE at present, which proves that the growth and doping of bulk GaN have made great progresses. Dislocation density in bulk GaN grown by HVPE decreases with thickness, leading to an increase in the electron mobility and an improvement of the optical properties. By using the precursor with good thermostability, Si doping is successfully realized in the hot-wall HVPE reactor with a concentration as high as 10^{19} cm^{-3}. The electrical properties of Ge-doped GaN is similar to that of Si-doped GaN, hence Ge doping is a promising choice for the growth of N-type GaN. Semi-insulating GaN with a resistivity above 10^{9} Ω·cm could be realized by compensating the background donor impurities by Fe doping. The structural and electronic properties of Fe in GaN are carefully studied, which could explain the compensation mechanism. The highly pure GaN could also be obtained using a quartz-free HVPE reactor.

However, there are still some problems concern with doping of GaN. In the case of Si doping, the donor concentration is limited by the tensile stress and morphology deterioration at elevated Si concentration. Ge doping is an appropriate method to further increase the upper limit of carrier concentration, but the V-shaped pits in the heavily Ge-doped GaN are current leakage channels. In order to increase the resistivity of Fe-doped GaN, more and more Fe impurities are incorporated. However, the excess Fe impurities could lead to various problems which is harmful to the performance of devices. Elimination of the defects in heavily doped GaN is a big challenge to realize industrial applications. HPSI GaN points out a new way to solve the problems above.

Acknowledgments

Thanks to Mrs. Zheng Shu-Nan, Gu Hong, Zhang Min, Tian Fei-Fei, Mr. Liu Zong-Liang, Huang Jun, Su Xu-Jun, and Shi Lin, for their contributions in characterization and discussion. Thanks to Mr. Huang Zeng-Li from the Vacuum Interconnected Nano-X Research Facility for his effort in sample preparation. Thanks to Mr. Xu, Lin, Zhao Mao-Mao, Jin Chao, and Zhang Zhi-Qiang from Nanowin Corporation for their devotions to GaN growth and doping.

References

[1] Miyoshi T, Masui S, Okada T, Yanamoto T, Kozaki T, Nagahama S-i and Mukai T 2009 *Appl. Phys. Express* **2** 062201
[2] Okur S, Shimada R, Zhang F, Hafiz S D A, Lee J, Avrutin V, Morkoc H, Franke A, Bertram F, Christen J and Oezguer U 2013 *Jpn. J. Appl. Phys.* **52** Unsp 08JH03
[3] Meyer D J, Deen D A, Storm D F, Ancona M G, Katzer D S, Bass R, Roussos J A, Downey B P, Binari S C, Gougousi T, Paskova T, Preble E A and Evans K R 2013 *IEEE Electron Dev. Lett.* **34** 199
[4] Storm D F, Katzer D S, Roussos J A, Mittereder J A, Bass R, Binari S C, Hanser D, Preble E A and Evans K R 2007 *J. Cryst. Growth* **301** 429
[5] Liu X, Liu Q, Li C, Wang J, Yu W, Xu K and Ao J P 2017 *Jpn. J. Appl. Phys.* **56** 026501
[6] Gu H, Hu C, Wang J, Lu Y, Ao J P , Tian F, Zhang Y, Wang M, Liu X and Xu K 2019 *J. Alloys Compd.* **780** 476
[7] Gu H, Tian F, Zhang C, Xu K, Wang J, Chen Y, Deng X and Liu X 2019 *Nanoscale Res. Lett.* **14** 40
[8] Liu Z, Wang J, Gu H, Zhang Y, Wang W, Xiong R and Xu K 2019 *AIP Adv.* **9** 055016
[9] Ji X, Dong W, Zhang Y, Wang J and Xu k 2019 *Chin. Phys. B* **28** 067701
[10] Mulligan P, Wang J and Cao L 2013 *Nucl. Instrum. Method A* **719** 13
[11] Fan Y, Xu K, Liu Z, Xu G, Zhong H, Huang Z, Zhang Y and Wang J 2017 *Jpn. J. Appl. Phys.* **56** 050307
[12] Fu K, Yu G, Yao C, Wang G, Lu M and Zhang G 2011 *Phys. Status Solidi-R* **5** 187
[13] Hibberd M T, Frey V, Spencer B F, Mitchell P W, Dawson P, Kappers M J, Oliver R A, Humphreys C J and Graham D M 2016 *Solid State Commun.* **247** 68

[14] Harima H 2002 *J. Phys.-Condens. Matter* **14** 967
[15] Xu K, Wang J F and Ren G Q 2015 *Chin. Phys. B* **24** 066105
[16] Motoki K, Okahisa T, Matsumoto N, Matsushima M, Kimura H, Kasai H, Takemoto K, Uematsu K, Hirano T, Nakayama M, Nakahata S, Ueno M, Hara D, Kumagai Y, Koukitu A and Seki H 2001 *Jpn. J. Appl. Phys.* **40** L140
[17] Fujikura H, Yoshida T, Shibata M and Otoki Y 2017 *Conference on Gallium Nitride Materials and Devices XII*, January 30–February 2, 2017, San Francisco, USA, p. 1010403
[18] Yoshida T, Imanishi M, Kitamura T, Otaka K, Imade M, Shibata M and Mori Y 2017 *Phys. Status Solidi B* **254** 1600671
[19] Gu H, Ren G, Zhou T, Tian F, Xu Y, Zhang Y, Wang M, Wang J and Xu K 2016 *J. Cryst. Growth* **436** 76
[20] Fan Y, Liu Z, Xu G, Zhong H, Huang Z, Zhang Y, Wang J and Xu K 2014 *Appl. Phys. Lett.* **105** 062108
[21] Lu M, Zhang G G, Fu K and Yu G H 2010 *Chin. Phys. Lett.* **27** 052901
[22] Yao C, Fu K, Wang G, Yu G and Lu M 2012 *Phys. Status Solidi A* **209** 204
[23] Usui A, Sunakawa H, Kuroda N, Kimura A, Sakai A and Yamaguchi A A 1998 *2nd International Symposium on Blue Laser and Light Emitting Diodes* (2nd ISBLLED), September 29–October 2, 1998, Chiba, Japan, pp. 17–21
[24] Iwinska M, Sochacki T, Amilusik M, Kempisty P, Lucznik B, Fijalkowski M, Litwin-Staszewska E, Smalc-Koziorowska J, Khapuridze A, Staszczak G, Grzegory I and Bockowski M 2016 *J. Cryst. Growth* **456** 91
[25] Hofmann P, Krupinski M, Habel F, Leibiger G, Weinert B, Eichler S and Mikolajick T 2016 *J. Cryst. Growth* **450** 61
[26] Oshima Y, Yoshida T, Watanabe K and Mishima T 2010 *J. Cryst. Growth* **312** 3569
[27] Zvanut M E, Dashdorj J, Freitas J A, Glaser E R, Willoughby W R, Leach J H and Udwary K 2016 *J. Electron. Mater.* **45** 2692
[28] Vaudo R P, Xu X P, Salant A, Malcarne J and Brandes G R 2003 *Phys. Status Solidi A-Appl. Res.* **200** 18
[29] Richter E, Gridneva E, Weyers M and Traenkle G 2016 *J. Cryst. Growth* **456** 97
[30] Zhang R and Kuech T F 1998 *Appl. Phys. Lett.* **72** 1611
[31] Iwinska M, Piotrzkowski R, Litwin-Staszewska E, Sochacki T, Amilusik M, Fijalkowski M, Lucznik B and Bockowski M 2017 *Appl. Phys. Express* **10** 011003
[32] Richter E, Hennig C, Zeimer U, Wang L, Weyers M and Tränkle G 2006 *Phys. Status Solidi A* **203** 1658
[33] Oshima Y, Yoshida T, Eri T, Shibata M and Mishima T 2006 *Jpn. J. Appl. Phys.* **45** 7685
[34] Foronda H M, Romanov A E, Young E C, Roberston C A, Beltz G E and Speck J S 2016 *J. Appl. Phys.* **120** 035104
[35] Xie J Q, Mita S, Rice A, Tweedie J, Hussey L, Collazo R and Sitar Z 2011 *Appl. Phys. Lett.* **98** 202101
[36] Fritze S, Dadgar A, Witte H, Bugler M, Rohrbeck A, Blasing J, Hoffmann A and Krost A 2012 *Appl. Phys. Lett.* **100** 122104
[37] Markurt T, Lymperakis L, Neugebauer J, Drechsel P, Stauss P, Schulz T, Remmele T, Grillo V, Rotunno E and Albrecht M 2013 *Phys. Rev. Lett.* **110** 036103
[38] Nakamura S, Mukai T and Senoh M 1992 *Jpn. J. Appl. Phys.* **31** 2883
[39] Kirste R, Hoffmann M P, Sachet E, Bobea M, Bryan Z, Bryan I, Nenstiel C, Hoffmann A, Maria J P, Collazo R and Sitar Z 2013 *Appl. Phys. Lett.* **103** 242107
[40] Gotz W, Kern R S, Chen C H, Liu H, Steigerwald D A and Fletcher R M 1999 *Mater. Sci. Eng. B-Solid* **59** 211
[41] Wieneke M, Witte H, Lange K, Feneberg M, Dadgar A, Blasing J, Goldhahn R and Krost A 2013 *Appl. Phys. Lett.* **103** 012103
[42] Kondo H, Oda S, Ogawa M and Zaima S 2008 *3rd International SiGe, Ge and Related Compounds Symposium*, October 12–17, 2008, Honolulu, USA, p. 717
[43] Nenstiel C, Bugler M, Callsen G, Nippert F, Kure T, Fritze S, Dadgar A, Witte H, Blasing J, Krost A and Hoffmann A 2015 *Phys. Status Solidi-R* **9** 716
[44] Xie J Q, Mita S, Hussey L, Rice A, Tweedie J, LeBeau J, Collazo R and Sitar Z 2011 *Appl. Phys. Lett.* **99** 141916
[45] Iwinska M, Takekawa N, Ivanov V Y, Amilusik M, Kruszewski P, Piotrzkowski R, Litwin-Staszewska E, Lucznik B, Fijalkowski M, Sochacki T, Teisseyre H, Murakami H and Bockowski M 2017 *J. Cryst. Growth* **480** 102
[46] Sang L W, Ren B, Sumiya M, Liao M Y, Koide Y, Tanaka A, Cho Y J, Harada Y, Nabatame T, Sekiguchi T, Usami S, Honda Y and Amano H 2017 *Appl. Phys. Lett.* **111** 122102
[47] Le L C, Zhao D G, Jiang D S, Li L, Wu L L, Chen P, Liu Z S, Li Z C, Fan Y M, Zhu J J, Wang H, Zhang S M and Yang H 2012 *Appl. Phys. Lett.* **101** 252110
[48] Hofer A, Benstetter G, Biberger R, Leirer C and Bruderl G 2013 *Thin Solid Films* **544** 139
[49] Montes Bajo M, Hodges C, Uren M J and Kuball M 2012 *Appl. Phys. Lett.* **101** 033508
[50] Puzyrev Y S, Schrimpf R D, Fleetwood D M and Pantelides S T 2015 *Appl. Phys. Lett.* **106** 053505
[51] Axelsson O, Billstrom N, Rorsman N and Thorsell M 2016 *IEEE Microw. Wirel. Compon. Lett.* **26** 31
[52] Oshimura Y, Takeda K, Sugiyama T, Iwaya M, Kamiyama S, Amano H, Akasaki I, Bandoh A and Udagawa T 2010 *8th International Conference on Nitride Semiconductors (ICNS)*, October 18–23, 2009, Jeju, South Korea, p. 1974
[53] Martin G M, Farges J P, Jacob G, Hallais J P and Poiblaud G 1980 *J. Appl. Phys.* **51** 2840
[54] Jenny J R, Malta D P, Muller S G, Powell A R, Tsvetkov V F, Hobgood H M, Glass R C and Carter C H 2003 *J. Electron. Mater.* **32** 432
[55] Kizilyalli I C, Edwards A P, Aktas O, Prunty T and Bour D 2015 *IEEE T. Electron. Dev.* **62** 414
[56] Fujikura H, Konno T, Yoshida T and Horikiri F 2017 *Jpn. J. Appl. Phys.* **56** 085503
[57] Maruska H P and Tietjen J J 1969 *Appl. Phys. Lett.* **15** 327
[58] Lee M, Ahn C W, Vu T K O, Lee H U, Kim E K and Park S 2019 *Sci. Rep.-UK* **9** 7128
[59] Park S S, Park I W and Choh S H 2000 *Jpn. J. Appl. Phys. Part. 2-Letters* **39** L1141
[60] Wong W S, Sands T and Cheung N W 1998 *Appl. Phys. Lett.* **72** 599
[61] Kelly M K, Vaudo R P, Phanse V M, Gorgens L, Ambacher O and Stutzmann M 1999 *Jpn. J. Appl. Phys. Part. 2-Letters* **38** L217
[62] Usui A, Sunakawa H, Sakai A and Yamaguchi A A 1997 *Jpn. J. Appl. Phys. Part. 2-Letters* **36** L899
[63] Sakai A, Sunakawa H and Usui A 1997 *Appl. Phys. Lett.* **71** 2259
[64] Motoki K, Okahisa T, Nakahata S, Matsumoto N, Kimura H, Kasai H, Takemoto K, Uematsu K, Ueno M, Kumagai Y, Koukitu A and Seki H 2002 *J. Cryst. Growth* **237** 912
[65] Oshima Y, Eri T, Shibata M, Sunakawa H, Kobayashi K, Ichihashi T and Usui A 2003 *Jpn. J. Appl. Phys. Part. 2-Letters* **42** L1
[66] Liu J, Huang J, Gong X, Wang J, Xu K, Qiu Y, Cai D, Zhou T, Ren G and Yang H 2011 *Crystengcomm* **13** 5929
[67] Vetterhoffer J and Weber J 1996 *Phys. Rev. B* **53** 12835
[68] Wu S, Yang X, Zhang H, Shi L, Zhang Q, Shang Q, Qi Z, Xu Y, Zhang J, Tang N, Wang X, Ge W, Xu K and Shen B 2018 *Phys. Rev. Lett.* **121** 145505
[69] Reshchikov M A and Morkoc H 2005 *J. Appl. Phys.* **97** 061301
[70] Shi J Y, Yu L P, Wang Y Z, Zhang G Y and Zhang H 2002 *Appl. Phys. Lett.* **80** 2293
[71] Ng H M, Doppalapudi D, Moustakas T D, Weimann N G and Eastman L F 1998 *Appl. Phys. Lett.* **73** 821
[72] Weimann N G, Eastman L F, Doppalapudi D, Ng H M and Moustakas T D 1998 *J. Appl. Phys.* **83** 3656
[73] Zhao D G, Yang H, Zhu J J, Jiang D S, Liu Z S, Zhang S M, Wang Y T and Liang J W 2006 *Appl. Phys. Lett.* **89** 112106
[74] Abdel-Motaleb I M and Korotkov R Y 2005 *J. Appl. Phys.* **97** 093715
[75] Khromov S, Hemmingsson C, Monemar B, Hultman L and Pozina G 2014 *J. Appl. Phys.* **116** 223503
[76] Shalish I, Kronik L, Segal C, Rosenwaks Y, Shapira Y, Tisch U and Salzman J 1999 *Phys. Rev. B* **59** 9748
[77] Lyons J L, Janotti A and Van de Walle C G 2010 *Appl. Phys. Lett.* **97** 152108
[78] Neugebauer J and Van de Walle C G 1996 *Appl. Phys. Lett.* **69** 503
[79] Chen H M, Chen Y F, Lee M C and Feng M S 1997 *Phys. Rev. B* **56** 6942
[80] Elsner J, Jones R, Heggie M I, Sitch P K, Haugk M, Frauenheim T, Öberg S and Briddon P R 1998 *Phys. Rev. B* **58** 12571
[81] Kang T S, Ren F, Gila B P, Pearton S J, Patrick E, Cheney D J, Law M and Zhang M L 2015 *J. Vac. Sci. Technol. B* **33** 061202

[82] Gu H, Ren G, Zhou T, Tian F, Xu Y, Zhang Y, Wang M, Zhang Z, Cai D, Wang J and Xu K 2016 *J. Alloy. Compd.* **674** 218

[83] Valente G, Cavallotti C, Masi M and Carra S 2001 *J. Cryst. Growth* **230** 247

[84] Hofmann P, Roder C, Habel F, Leibiger G, Beyer F C, Gartner G, Eichler S and Mikolajick T 2016 *J. Phys. D* **49** 075502

[85] Richter E, Stoica T, Zeimer U, Netzel C, Weyers M and Trankle G 2013 *J. Electron. Mater.* **42** 820

[86] Fomin A V, Nikolaev A E, Nikitina I P, Zubrilov A S, Mynbaeva M G, Kuznetsov N I, Kovarsky A P and Ber B J 2001 *Phys. Status Solidi A-Appl. Res.* **188** 433

[87] Noda S, Tanabe K, Yahiro T, Osawa T and Komiyama H 2004 *J. Electrochem. Soc.* **151** C399

[88] Romano L T, Van de Walle C G, Ager J W, Gotz W and Kern R S 2000 *J. Appl. Phys.* **87** 7745

[89] Dadgar A, Veit P, Schulze F, Bläsing J, Krtschil A, Witte H, Diez A, Hempel T, Christen J, Clos R and Krost A 2007 *Thin Solid Films* **515** 4356

[90] Romanov A E and Speck J S 2003 *Appl. Phys. Lett.* **83** 2569

[91] Brunner F, Mogilatenko A, Knauer A, Weyers M and Zettler J T 2012 *J. Appl. Phys.* **112** 033503

[92] Moram M A, Kappers M J, Massabuau F, Oliver R A and Humphreys C J 2011 *J. Appl. Phys.* **109** 073509

[93] Follstaedt D M, Lee S R, Allerman A A and Floro J A 2009 *J. Appl. Phys.* **105** 083507

[94] Usikov A, Kovalenkov O V, Mastro M M, Tsvetkov D V, Pechnikov A I, Soukhoveev V A, Shapovalova Y V and Gainer G H 2003 *Symposium on GaN and Related Alloys held at the* 2002 *MRS Fall Meeting*, December 2–6, 2002, Boston, USA, p. 231

[95] Munkholm A, Thompson C, Murty M V R, Eastman J A, Auciello O, Stephenson G B, Fini P, DenBaars S P and Speck J S 2000 *Appl. Phys. Lett.* **77** 1626

[96] Tanaka S, Takeuchi M and Aoyagi Y 2000 *Jpn. J. Appl. Phys. Part. 2-Lett.* **39** L831

[97] Neugebauer J 2003 *Phys. Stat. Sol. (c)* 1651

[98] Neugebauer J, Zywietz T K, Scheffler M, Northrup J E, Chen H and Feenstra R M 2003 *Phys. Rev. Lett.* **90** 056101

[99] Rosa A L, Neugebauer J, Northrup J E, Lee C D and Feenstra R M 2002 *Appl. Phys. Lett.* **80** 2008

[100] Oshima Y, Yoshida T, Eri T, Shibata M and Mishima T 2007 *International Workshop on Nitride Semiconductors 2006 (IWN 2006)*, October 22–27, 2006, Kyoto, Japan, p. 2215

[101] Schörmann J, Hille P, Schäfer M, Müßener J, Becker P, Klar P J, Kleine-Boymann M, Rohnke M, Mata M d l, Arbiol J, Hofmann D M, Teubert J and Eickhoff M 2013 *J. Appl. Phys.* **114** 103505

[102] Walsh A, Da Silva J L F and Wei S H 2008 *Phys. Rev. B* **78** 075211

[103] Wu J, Walukiewicz W, Shan W, Yu K M, Ager J W, Haller E E, Lu H and Schaff W J 2002 *Phys. Rev. B* **66** 201403

[104] Cantu P, Wu F, Waltereit P, Keller S, Romanov A E, Mishra U K, DenBaars S P and Speck J S 2003 *Appl. Phys. Lett.* **83** 674

[105] Yamane K, Matsubara T, Yamamoto T, Okada N, Wakahara A and Tadatomo K 2016 *J. Appl. Phys.* **119** 045707

[106] Dadgar A, Blasing J, Diez A and Krost A 2011 *Appl. Phys. Express* **4** 011001

[107] Voronenkov V, Bochkareva N, Gorbunov R, Latyshev P, Lelikov Y, Rebane Y, Tsyuk A, Zubrilov A and Shreter Y 2013 *Jpn. J. Appl. Phys.* **52** 08JE14

[108] Leach J H, Wu M, Ni X, Li X, Xie J, Özgür Ü Morkoç H, Paskova T, Preble E, Evans K R and Lu C Z 2010 *Appl. Phys. Lett.* **96** 102109

[109] Kubota M, Onuma T, Ishihara Y, Usui A, Uedono A and Chichibu S F 2009 *J. Appl. Phys.* **105** 083542

[110] Gladkov P, Humlicek J, Hulicius E, Simecek T, Paskova T and Evans K 2010 *J. Cryst. Growth* **312** 1205

[111] Malguth E, Hoffmann A and Phillips M R 2008 *J. Appl. Phys.* **104**

[112] Ohba Y and Hatano A 1994 *J. Cryst. Growth* **145** 214

[113] Heikman S, Keller S, Mates T, DenBaars S P and Mishra U K 2003 *J. Cryst. Growth* **248** 513

[114] Malguth E, Hoffmann A, Gehlhoff W, Gelhausen O, Phillips M R and Xu X 2006 *Phys. Rev. B* **74** 165202

[115] Maier K, Kunzer M, Kaufmann U, Schneider J, Monemar B, Akasaki I and Amano H 1994 17*th International Conference on Defects in Semiconductors*, July 18–23, 1993, Gmunden, Austria, p. 93

Maier K, Kunzer M, Kaufmann U, Schneider J, Monemar B, Akasaki I and Amano H 1994 17th International Conference on Defects in Semiconductors, July 18-23, 1993, Gmunden, Austria, p. 93 DOI: https://doi.org/10.4028/www.scientific.net/MSF.143-147.93

[116] Heitz R, Maxim P, Eckey L, Thurian P, Hoffmann A, Broser I, Pressel K and Meyer B K 1997 *Phys. Rev. B* **55** 4382

[117] Malguth E, Hoffmann A and Xu X 2006 *Phys. Rev. B* **74** 165201

[118] Zhang M, Zhou T F, Zhang Y M, Li B, Zheng S N, Huang J, Sun Y P, Ren G Q, Wang J F, Xu K and Yang H 2012 *Appl. Phys. Lett.* **100** 041904

[119] Zhang Y, Wang J, Zheng S, Cai D, Xu Y, Wang M, Hu X, Zhao M and Xu K 2019 *Appl. Phys. Express* **12** 074002

[120] Walsh A, Da Silva J L F and Wei S H 2008 *Phys. Rev. B* **78** 075211

[121] Yoshikawa M, Kunzer M, Wagner J, Obloh H, Schlotter P, Schmidt R, Herres N and Kaufmann U 1999 *J. Appl. Phys.* **86** 4400

[122] Xu S R, Hao Y, Zhang J C, Cao Y R, Zhou X W, Yang L A, Ou X X, Chen K and Mao W 2010 *J. Cryst. Growth* **312** 3521

[123] Cruz S C, Keller S, Mates T E, Mishra U K and DenBaars S P 2009 *J. Cryst. Growth* **311** 3817

[124] Tanaka T, Kaneda N, Mishima T, Kihara Y, Aoki T and Shiojima K 2015 *Jpn. J. Appl. Phys.* **54** 041002

[125] Fujikura H, Konno T, Yoshida T and Horikiri F 2017 *Jpn. J. Appl. Phys.* **56** 085503

[126] Tompkins R P, Khan M R, Green R, Jones K A and Leach J H 2016 *J. Mater. Sci.: Mater. Electron.* **27** 6108

[127] Polyakov A Y, Smirnov N B, Govorkov A V, Yugova T G, Cox H, Usikov A S, Helava H and Makarov Y 2014 *J. Appl. Phys.* **115** 183706

[128] Sumiya M, Yoshimura K, Ohtsuka K and Fuke S 2000 *Appl. Phys. Lett.* **76** 2098

[129] Zywietz T K, Neugebauer J and Scheffler M 1999 *Appl. Phys. Lett.* **74** 1695

[130] Zywietz T, Neugebauer J and Scheffler M 1998 *Appl. Phys. Lett.* **73** 487

[131] Fichtenbaum N A, Mates T E, Keller S, DenBaars S P and Mishra U K 2008 *J. Cryst. Growth* **310** 1124